

POTENTIAL-DENSITY PAIRS FOR GALAXY DISCS WITH EXPONENTIAL OR SECH² VERTICAL PROFILE

WALTER DEHNEN*  AND SHERA JAFARITABAR

Astronomisches Rechen-Institut, Zentrum für Astronomie der Universität Heidelberg, Mönchhofstr. 12-14, 69120, Heidelberg, Germany

submitted October 7, 2024; accepted January 8, 2025

ABSTRACT

We present axially symmetric analytical potential-density pairs with surface density similar to the Miyamoto-Nagai model, but with more realistic vertical structure. Our models closely approximate an exponential, a sech², or a cored exponential vertical density profile. The latter profile has a density core of adjustable width, which provides more flexibility when modelling galaxy discs.

Subject headings: methods: analytical — galaxies: structure — galaxies: kinematics and dynamics

1. INTRODUCTION

Studies of the dynamics of the Milky Way and other disc galaxies often require models for the gravitational potential which should be realistic as well as easy to implement and compute. Unfortunately, these two goals appear mutually exclusive, since galactic discs have vertically near-exponential profiles (e.g. Jurić et al. 2008; Dobbie & Warren 2020; Mosenkov et al. 2021) for which no analytical models are known. In face of this dilemma, mainly two approaches have been used in practice: (1) numerical computation of gravitational potentials for observationally motivated density models (Kuijken & Dubinski 1995; Dehnen & Binney 1998), and (2) simple analytical disc models with unrealistic vertical profiles (Miyamoto & Nagai 1975, hereafter MN; Evans & Bowden 2014).

The vertical density profile of the widely used MN model deviates from the exponential profile in two ways. First, at large $|z|$ it decays only like the power law $|z|^{-5}$. This deviation is presumably benign in the sense that the resulting differences between the forces at large $|z|$, and hence the ensuing orbits, are relatively minor.

The second deviation of the MN model from a vertically exponential density profile occurs at small $|z|$, where the former exhibits a near-constant density core and declines only like z^2 , while the latter declines linearly in $|z|$. This difference translates to the vertical Taylor expansion of the potential at small $|z|$:

$$\Phi = \Phi_0 + \frac{1}{2}\nu^2 z^2 + \begin{cases} O(|z|^3) & \text{for an exponential,} \\ O(z^4) & \text{for a density core,} \end{cases} \quad (1)$$

where Φ_0 and ν denote the mid-plane value and the vertical epicycle frequency, respectively. Thus, the motion in a vertically exponential disc is much more strongly anharmonic than in a disc with density core, such as the MN model. This anharmonicity results in important dynamical effects, which are neglected when using the MN model. One effect is the presence of more orbital resonances owing to higher vertical orbital frequencies for an exponential disc. Another effect is more efficient vertical phase mixing, which in turn leads to a quick loss of vertical coherence of tidal debris from dissolving star clusters (Dehnen & Hasanuddin 2018) and to a faster winding

of phase-spirals in the z - v_z phase space, such as those observed in the Milky Way (Antoja et al. 2018).

A hybrid of the numerical and analytical approaches to disc modelling is to superimpose several MN models with parameters numerically determined to approximate a vertically exponential disc (Rojas-Niño et al. 2016 achieved $\sim 10\%$ accuracy). However, this does not completely solve the discrepancies at small and large z , since also the combination of several MN models has an, albeit small, density core and power-law fall-off at $z \rightarrow \pm\infty$.

In this study, we introduce novel analytical potentials for galactic discs, most properties of which at $z = 0$ are identical to a corresponding MN model, but which have vertical density profiles very close to exponential, sech², or a cored exponential profile. The models and their properties are derived in Sections 2 and 3, and assessed in Section 4, while Section 5 concludes our study.

2. MODIFYING THE KUZMIN DISC

The Kuzmin (1956) disc has gravitational potential

$$\Phi(R, z) = -\frac{GM}{X} \quad \text{with} \quad X \equiv \sqrt{R^2 + Z^2}, \quad (2)$$

where $Z = a + |z|$ with some scale length a , and mass density $\rho(R, z) = \Sigma(R)\delta(z)$ with surface density

$$\Sigma(R) = \frac{aM}{2\pi(R^2 + a^2)^{3/2}}. \quad (3)$$

Such a razor-thin mass distribution is not very realistic, but one can obtain more realistic models by setting

$$Z = a + \zeta(z) \quad (4)$$

with some function $\zeta(z)$ which in the limits $z \rightarrow \pm\infty$ approaches $|z|$, such that $\Phi \rightarrow -GM/\sqrt{R^2 + z^2}$ and the parameter M retains its meaning as the total mass.

The MN model is obtained from this recipe for $\zeta = \zeta_M \equiv \sqrt{z^2 + b^2}$ with scale height b . However, other useful but hitherto unknown modifiers $\zeta(z)$ may exist. In order to explore this possibility, we now investigate the general properties of these modified Kuzmin models and obtain conditions for the function $\zeta(z)$.

The mass density related via Poisson's equation is

$$\rho(R, z) = \frac{M}{4\pi X^3} \left[Z\zeta'' + \left(\frac{3Z^2}{X^2} - 1 \right) (1 - \zeta'^2) \right]. \quad (5)$$

*E-mail: walter.dehnen@uni-heidelberg.de

For $\zeta = |z|$, we have $\zeta' = \text{sign}(z)$ and $\zeta'' = 2\delta(z)$, such that equation (5) recovers the Kuzmin model as required. In order to avoid a razor-thin component, the function ζ must be C^2 , which for vertically symmetric discs implies $\zeta'(0) = 0$. In this case, it is useful to introduce

$$\xi(z) \equiv [1 - \zeta'^2(z)]/\zeta''(z), \quad (6)$$

such that the density can be written as

$$\rho(R, z) = \frac{M\zeta''}{4\pi} \left[\frac{Z - \xi}{X^3} + \frac{3\xi Z^2}{X^5} \right]. \quad (7)$$

For this to be non-negative everywhere, we first require that $\zeta'' \geq 0$ (which with the previous conditions implies $1 - \zeta'^2 \geq 0$ and $\xi \geq 0$). In this case $\rho \geq 0$ everywhere if $Z \geq \xi$. At $z = 0$, this reduces to $(a + \zeta)\zeta'' \geq 1$, which holds for any value $a \geq 0$ if $\zeta\zeta'' = 1$ at $z = 0$, is our final condition¹ for ζ , and implies $\xi(0) = \zeta_0 \equiv \zeta(0)$. For some models $Z < \xi$ and hence $\rho < 0$ at $z \neq 0$ is still possible for small a , as we see below.

To summarise, the function $\zeta(z)$ must satisfy the following conditions

1. $\zeta \rightarrow |z|$ as $z \rightarrow \pm\infty$.
2. ζ is C^2 with $\zeta'(0) = 0$ and $\zeta'' \geq 0$.
3. $\zeta''(0) = 1/\zeta_0$ with $\zeta_0 \equiv \zeta(0)$.

With these conditions, the properties of modified Kuzmin models with the same values for a and ζ_0 are identical in the mid-plane $z = 0$, regardless of their respective functions $\zeta(z)$. The potential in the mid-plane

$$\Phi(R, 0) = -\frac{GM}{\sqrt{R^2 + s^2}}, \quad (8)$$

equals that of a [Plummer \(1911\)](#) sphere with scale radius

$$s \equiv Z(0) = a + \zeta_0 \quad (9)$$

and is independent of ζ_0 (at given s), a property inherited by its radial derivatives, e.g. the circular speed curve.

The [MN](#) modifier $\zeta_M = \sqrt{z^2 + b^2}$ satisfies all our conditions and gives $\xi = \zeta$ and ([Miyamoto & Nagai 1975](#))

$$\rho_M(R, z) = \frac{M}{4\pi} \frac{b^2}{X^3(z^2 + b^2)} \left[\frac{a}{\sqrt{z^2 + b^2}} + \frac{3Z^2}{X^2} \right], \quad (10)$$

which at fixed R is near-constant for $|z| \ll b$ and declines like $|z|^{-5}$ at $|z| \rightarrow \infty$.

To construct other useful modifiers $\zeta(z)$, we observe from equation (5) that the vertical density profiles at some R are close to $\zeta''(z)$ at small $|z|$. We now consider models, constructed via a recipe given in [Appendix C](#), for which ζ'' is either exponential or sech^2 .

2.1. A (nearly) exponential vertical profile

A model with vertical profiles very close to exponential with scale height h is generated by the modifier

$$\zeta_E(z) = |z| + he^{-|z|/h}, \quad (11a)$$

for which

$$\zeta_E'' = h^{-1} e^{-|z|/h} \quad \text{and} \quad \xi_E = h(2 - e^{-|z|/h}). \quad (11b)$$

¹ In view of equation (4) and the freedom to choose $a \geq 0$, we can specify $\zeta_0 \equiv \zeta(0)$ without loss of generality.

The resulting density

$$\rho_E(R, z) = \frac{M}{4\pi} \frac{e^{-|z|/h}}{X^3} \left[\frac{Z}{h} + \left(\frac{3Z^2}{X^2} - 1 \right) (2 - e^{-|z|/h}) \right] \quad (12)$$

is close to exponential at small $|z|$, but in the mid-plane is identical to the [MN](#) model for the same s and $b = h$.

Since $\zeta_E - \xi_E < 0$ at $0 < |z| \lesssim 1.6h$ with a minimum of $h(\ln 2 - 1)$ at $|z|/h = \ln 2$, the density is negative near that minimum for $h/a > 1/(1 - \ln 2) \approx 3.26$ and non-monotonic for somewhat smaller h/a . However, for typical applications $h \ll a$ and no such behaviour occurs.

2.2. A vertical profile close to sech^2

A model with vertical profiles very close to sech^2 is generated by the modifier

$$\zeta_S(z) = z_0 + z_0 \ln \cosh \frac{z}{z_0}, \quad (13a)$$

such that

$$\zeta_S'' = \frac{1}{z_0} \text{sech}^2 \frac{z}{z_0} \quad \text{and} \quad \xi_S = z_0 \quad (13b)$$

and we find from equation (7)

$$\rho_S(R, z) = \frac{M}{4\pi X^3} \text{sech}^2 \frac{z}{z_0} \left[\frac{a}{z_0} + \ln \cosh \frac{z}{z_0} + \frac{3Z^2}{X^2} \right]. \quad (14)$$

Again, for the same value of s , the mid-plane density is identical to that of the near-exponential model for $h = z_0$ or the [MN](#) model for $b = z_0$. At $|z| \gg z_0$, $\text{sech}^2(z/z_0) \sim e^{-2|z|/z_0}$, such that $z_0 = 2h$ obtains exponential decay with scale height h , in which case the mid-plane density is about half of that of the exponential model.

Since $\zeta_S - \xi_S \geq 0$, $\rho_S \geq 0$ everywhere.

2.3. Cored exponential vertical profiles

The sech^2 profile, unlike the exponential but similar to the [MN](#) disc, has a density core: a region of near-constant density at low $|z|$. Comparing

$$\text{sech}^2 \frac{z}{2h} = 1 - \frac{z^2}{4h^2} + O(z^4) \quad (15)$$

to the simple cored exponential profile

$$e^{-\sqrt{z^2 + w^2}/h} \propto 1 - \frac{z^2}{2hw} + O(z^4), \quad (16)$$

suggests $w = 2h$ for the width of this core.

A cored exponential profile can be constructed as the difference of two exponentials with scale heights h and w , respectively. Using this approach, we extend the modifier ζ_E to include the parameter $w \in [0, h]$, generating models with cored exponential vertical profiles. For $w < h$,

$$\zeta_E = |z| + \frac{hw(h - w) + h^3 e^{-|z|/h} - w^3 e^{-|z|/w}}{h^2 - w^2}, \quad (17a)$$

$$\zeta_E' = \text{sign}(z) \left[1 - \frac{h^2 e^{-|z|/h} - w^2 e^{-|z|/w}}{h^2 - w^2} \right], \quad (17b)$$

$$\zeta_E'' = \frac{h e^{-|z|/h} - w e^{-|z|/w}}{h^2 - w^2} \propto 1 - \frac{z^2}{2hw} + O(|z|^3), \quad (17c)$$

which gives equations (11) for $w = 0$, while for $w = h$

$$\zeta_E = |z| + \frac{1}{2} \left[h + (3h + |z|) e^{-|z|/h} \right], \quad (18a)$$

$$\zeta'_E = \text{sign}(z) \left[1 - \frac{2h + |z|}{2h} e^{-|z|/h} \right], \quad (18b)$$

$$\zeta''_E = \frac{h + |z|}{2h^2} e^{-|z|/h} \propto 1 - \frac{z^2}{2h^2} + O(|z|^3). \quad (18c)$$

For these models, $\zeta_0 = h + w$, such that $s = a + h + w$. A limitation is that $w \leq h$ is required (for $w > h$, w and h simply swap their roles).

Again, non-monotonic vertical profiles or even $\rho < 0$ can occur for these models if $h \gtrsim a$.

2.4. Modified Toomre models?

Toomre (1963) introduced a family of razor-thin discs with surface densities $\Sigma \propto (R^2 + a^2)^{-k-1/2}$, which includes the Kuzmin disc for $k = 1$. These models can be modified in exactly the same way as the Kuzmin disc, and Miyamoto & Nagai (1975) gave the resulting relations for $\zeta = \zeta_M$ and $k = 1, 2, 3$. The density of the modified Toomre $k > 1$ models contains a term $\propto \zeta''(\zeta - \xi)/X^3$. For the MN modifier, $\xi = \zeta$ everywhere and this term vanishes identically, but for all other modifiers, this term either causes negative densities (for ζ_E) or prevents the density from decaying faster than for the $k = 1$ models at large R . Hence, there is little point to consider the modified $k > 1$ Toomre models.²

3. FURTHER ANALYTICAL PROPERTIES

The edge-on projected surface density $\Sigma = \int \rho \, dy$ is

$$\Sigma(x, z) = \frac{M\zeta''}{2\pi(x^2 + Z^2)} \left[Z + \frac{Z^2 - x^2}{x^2 + Z^2} \xi \right], \quad (19)$$

which in the mid-plane is again identical for models with different $\zeta(z)$ as long as they have the same values for s and ζ_0 . The surface density $\Sigma = \int \rho \, dz$ for the face-on projection cannot be expressed in closed form, but requires numerical treatment (see Appendix A).

The circular frequency and the radial and vertical epicycle frequencies are, respectively,

$$\Omega^2(R) = \frac{1}{R} \frac{\partial \Phi}{\partial R} \Big|_{z=0} = \frac{GM}{(R^2 + s^2)^{3/2}}, \quad (20a)$$

$$\kappa^2(R) = 4\Omega^2 + R \frac{d\Omega^2}{dR} = \frac{R^2 + 4s^2}{R^2 + s^2} \Omega^2(R), \quad (20b)$$

$$\nu^2(R) = \frac{\partial^2 \Phi}{\partial z^2} \Big|_{z=0} = \frac{s}{\zeta_0} \Omega^2(R). \quad (20c)$$

The first two do not depend on the vertical structure of the disc, but only on the scale radius s (and total mass M), while the vertical epicycle frequency ν depends on the vertical structure through ζ_0 and is $\sqrt{s/\zeta_0}$ times larger than Ω .

² Actually, the $k > 2$ MN models suffer from a similar issue: their density only decays like R^{-5} at large R , the same as the $k = 2$ model but shallower than the razor-thin $k > 2$ Toomre discs.

The vertical Jeans equation for axially symmetric systems reads (e.g. Binney & Tremaine 2008, eq. 4.222b)

$$\frac{1}{R} \frac{\partial(R\rho\overline{v_R v_z})}{\partial R} + \frac{\partial(\rho\sigma_z^2)}{\partial z} = -\rho \frac{\partial \Phi}{\partial z}, \quad (21)$$

where over-lining indicates a local average and $\sigma_z^2 \equiv \overline{v_z^2}$ is the vertical velocity dispersion of the population with density ρ . The mixed term $\overline{v_R v_z}$ vanishes if the distribution function of that population depends only on the classical integrals energy E and angular momentum L_z (Nagai & Miyamoto 1976; in this case also $\sigma_R = \sigma_z$) and otherwise tends to be small, in particular for $z \ll R$. When neglecting this term, equation (21) has solution

$$\rho\sigma_z^2(R, z) = \int_z^\infty \rho \frac{\partial \Phi}{\partial z} \, dz. \quad (22)$$

In the case of self-gravitating systems ($4\pi G\rho = \nabla^2 \Phi$), equation (22) gives for the modified Kuzmin models

$$\rho\sigma_z^2(R, z) = \frac{GM^2}{8\pi} \frac{Z^2}{X^6} (1 - \zeta'^2) \quad (23)$$

(see Appendix B for a derivation; for the MN model equivalent expressions were given by Nagai & Miyamoto and Ciotti & Pellegrini 1996), such that with equation (5)

$$\sigma_z^2 = \frac{GM}{2X^3} \left[\frac{1}{Z} \left(\frac{1}{\xi} - \frac{1}{Z} \right) + \frac{3}{X^2} \right]^{-1}. \quad (24)$$

4. ASSESSING THE MODELS

We now assess four exemplary modified Kuzmin models: the exponential model with scale height h , the sech² model with $z_0 = 2h$, the cored exponential model with $w = 0.5h$, and the MN model with $b = 1.5h$. We compare these models at the same value for their respective scale radius s (rather than scale length a), such that the mid-plane potentials (as well as circular speed and the frequencies Ω and κ) are identical between the models. The latter two models also have the same value for ζ_0 such that all their properties at $z = 0$ are identical. In all figures, we use units for which $G = M = s = 1$.

4.1. Vertical density profiles

In Fig. 1, we plot the vertical density profiles of the models for three different values of the scale-height parameter h and at three different radii R . We first focus on the near-exponential models (red). Their density profiles appear linear in the $\log \rho$ vs. z presentation of Fig. 1, implying an exponential decay. However, the slopes at different radii R are not exactly the same but become shallower for larger R (corresponding to a flaring disc), in particular for larger h . Moreover, as already discussed, the profiles are not exactly exponential, but display some deviation, most strongly at $|z| < h$.

In order to assess these deviations, we plot in Fig. 2 the local exponential scale height

$$h_{\text{local}} = \left| \frac{\partial \ln \rho}{\partial z} \right|^{-1} \quad (25)$$

as function of z . For a perfectly exponential profile, h_{local} would be constant, namely $h_{\text{local}} = h$. The (nearly) exponential model (red) deviates slightly from these ideals,

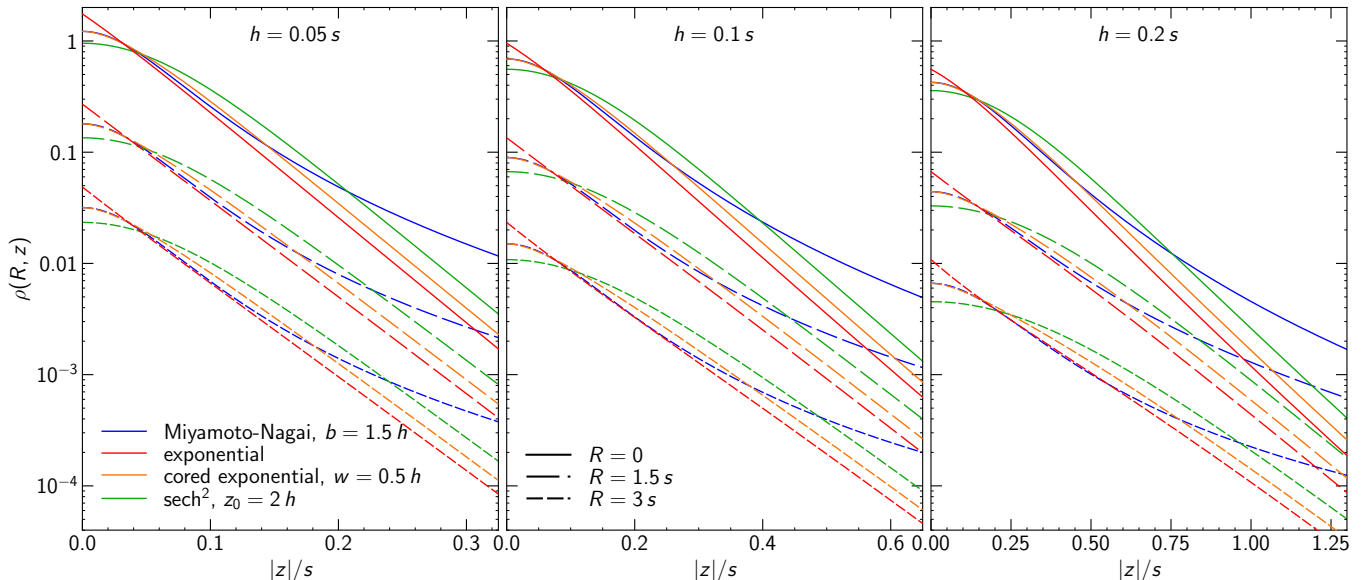


FIG. 1.— Vertical density profiles for various modified Kuzmin models of Section 2 for different exponential scale heights h and different radii R , as indicated. The Miyamoto-Nagai model with $b = 1.5h$ approximates $\exp(-|z|/h)$ for $0.5h \lesssim |z| \lesssim 3h$ and largely overlaps at $|z| \lesssim 2h$ with the cored exponential model with $w = 0.5h$. Note the different abscissa scales.

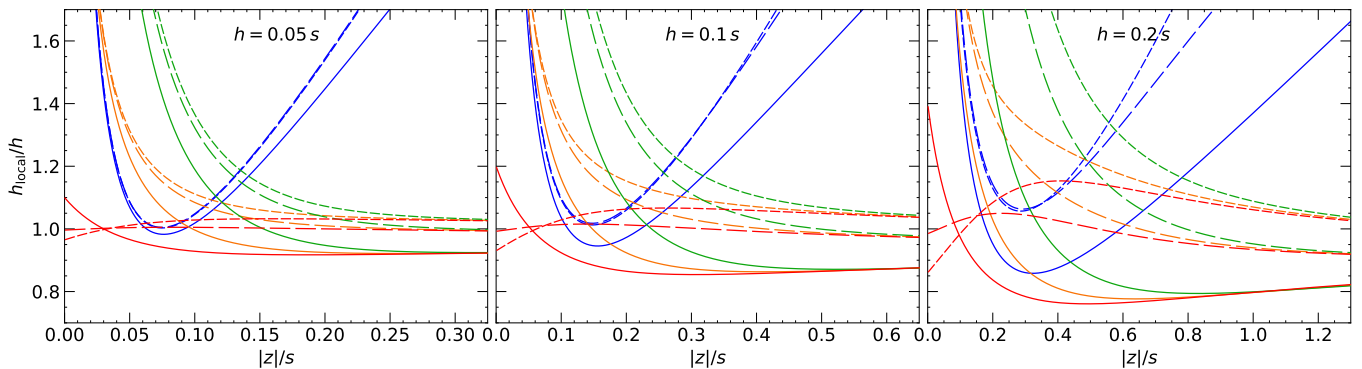


FIG. 2.— Vertical profiles of the local exponential scale height h_{local} (equation 25) for the same models and radii as in Fig. 1 (represented with the same colours and line styles). For a perfectly exponential vertical density profile, h_{local} is constant. For the exponential and sech^2 models, $h_{\text{local}} \rightarrow h$ for $z \rightarrow \pm\infty$ at fixed R .

the stronger the larger h . When modelling the thin stellar disc of, say, the Milky Way, $h \simeq 0.05s$ is a reasonable choice³, for which these deviations are quite small.

Next, we consider the cored exponential (orange in Fig. 1) and sech^2 (green) models. At large z , their vertical profiles, plotted in Fig. 1, have the same slope and hence scale height as the exponential model, while $h_{\text{local}} \rightarrow \infty$ at $z \rightarrow 0$ as a consequence of the density core.

Finally, we also plot in Figs. 1 and 2 the MN models for $b = 1.5h$ (blue), which for $|z| \lesssim 3h$ are very similar to the cored exponential models with $w = 0.5h$, but deviate increasingly at larger $|z|$, where they only decay as $|z|^{-5}$.

4.2. Projected density

In the limit $h \rightarrow 0$ (or $b \rightarrow 0$) the modified Kuzmin models approach the Kuzmin disc and hence their face-

³ The surface density of these models is close to that of the Kuzmin disc, whose local exponential scale length h_R (computed equivalently to h_{local}) has the minimum $2s/3$ at $R = s$. Hence, one may assign a scale radius for a modified Kuzmin model as $s = 1.5h_R$. Thus, $h = 0.05s$ corresponds to $h_R/h_z = 3.2\text{kpc}/240\text{pc}$.

on projected surface density $\Sigma(R) = \int \rho dz$ converges towards equation (3). Therefore, we expect $\Sigma(R)$ to deviate only slightly from that of the Kuzmin disc as long as $h \ll s$.

In Fig. 3, we plot the ratio of $\Sigma(R)$ (computed numerically as detailed in Appendix A) to the surface density (3) of the Kuzmin disc with the same scale radius s . We find indeed that these ratios are close to unity for small h , but deviate from this with increasing h . In each case, the model with surface density closest to the Kuzmin disc is the exponential model, while cored models deviate more, the stronger the more cored they are. However, at the same value for h (so that the models have comparable exponential scale heights) the surface density between the models are very similar in the sense that they differ much more from the Kuzmin disc than from each other.

In Fig. 4, we plot the contours of the edge-on projected densities (equation 19) for the choice $h = 0.1s$. The models differ in two aspects. First, the shape of the contours at $z = 0$ is pointed for the exponential profile but rounded for all the cored profiles (this difference may

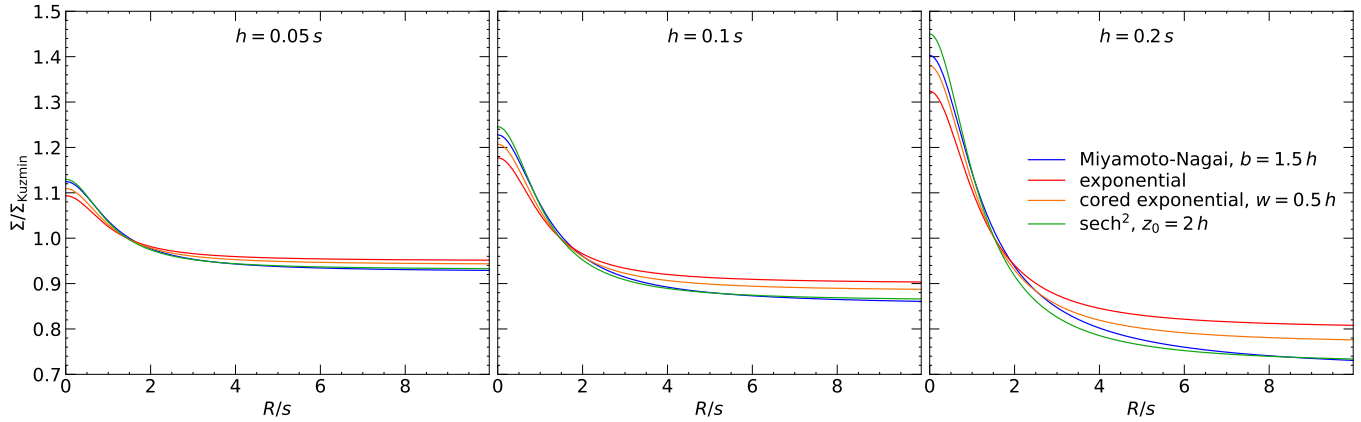


FIG. 3.— Radial profiles of the ratio of the (face-on projected) surface density $\Sigma(R)$ to that of the **Kuzmin** disc (equation 3 with $a = s$) for the same models as in Fig. 1.

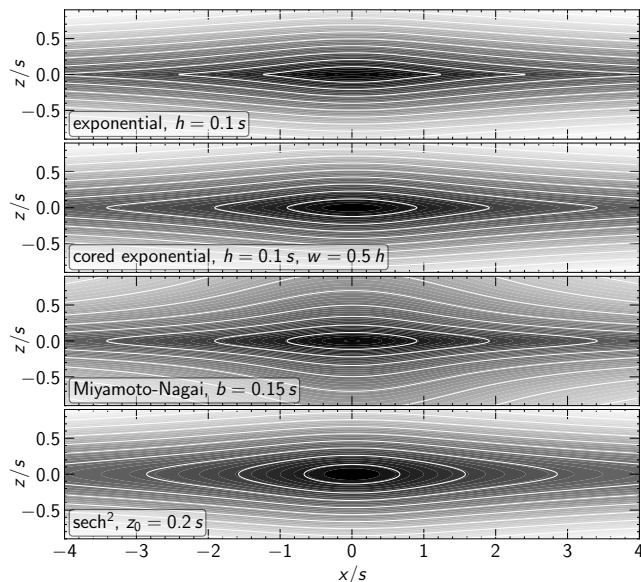


FIG. 4.— Contours (logarithmically spaced) of the edge-on projected density for the same models as shown in Fig. 1. Contour levels and grey-scale map are the same for all models. Note the behaviour of the contours near $z = 0$ and towards large $|z|$.

in practice be hard to observe owing to internal dust obscuration). Second, the projected density of the **MN** disc declines much more slowly at large $|z|$.

4.3. Vertical gravity and orbital frequency

As emphasised in the introduction, an important difference between the **MN** disc and a vertically exponential disc is the behaviour of gravity at small heights z . To demonstrate this, we plot in the upper three panels of Fig. 5 the potential, acceleration, and acceleration over height as function of height for the same four models. While the potentials look rather similar, the vertical force of the exponential model at small $|z|$ is clearly stronger than for the cored models, an immediate consequence of the larger amount of mass at near $z = 0$. This difference to the cored models is more obvious in the plots of the ratio $(\partial\Phi/\partial z)/z$ of acceleration to height, which for exactly harmonic potentials is constant. The cored models indeed possess a small region of near-constant $(\partial\Phi/\partial z)/z$ around the mid-plane.

In the bottom panel of Fig. 5, we plot the approxima-

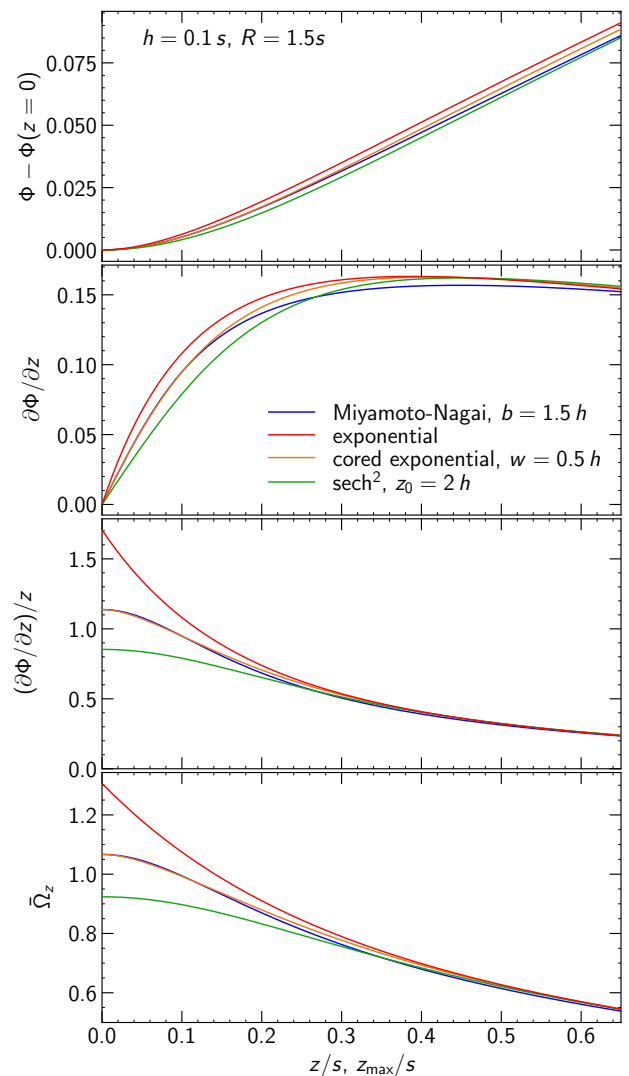


FIG. 5.— Profiles (from top to bottom) of the gravitational potential, the (negative) acceleration, and acceleration over height z as function of height, as well as that of the approximation (26) of the vertical orbital frequency as function of the maximal orbital height z_{\max} . Models are the same as in other figures with $h = 0.1s$ and at $R = 1.5s$ (e.g. the middle panels of Figs. 1 and 2, which also have the same x -axis scale). Units are such that $GM = 1 = s$.

tion

$$\bar{\Omega}_z(R, z_{\max}) = \frac{\pi}{2} \int_0^{z_{\max}} \frac{dz}{\sqrt{2[\Phi(R, z_{\max}) - \Phi(R, z)]}} \quad (26)$$

for the vertical orbital frequency Ω_z as function of maximum orbital height z_{\max} ⁴. Its profiles are reminiscent of those for $(\partial\Phi/\partial z)/z$ (which at $z \rightarrow 0$ converges to $\nu^2 = \bar{\Omega}_z^2(z_{\max} = 0)$), in particular, for the cored models $\bar{\Omega}_z$ is near-constant at small z_{\max} , while the exponential disc shows no such behaviour. The degree of orbital phase mixing is determined by the gradient $d\Omega_z/dz_{\max}$, which for the exponential disc is largest at small z , where it vanishes for the cored models. This implies that the behaviour of vertical phase mixing, which drives the evolution of the z - v_z phase-spiral in the Milky Way (Binney & Schönrich 2018), is fundamentally different between these two models.

We also see from the bottom panel of Fig. 5 that at small z_{\max} an exponential profile reaches larger frequencies Ω_z than a cored profile with the same exponential scale height. This has important implications for the existence of the $\Omega_z:\Omega_r = 2:1$ and $3:2$ orbital resonances, which, depending on the width of the core, may not occur in cored models or only over a smaller radial range than for the purely exponential models.

4.4. Velocity dispersion

For small heights $|z|$, i.e. for most disc stars, the vertical Jeans equation (21) is well approximated by neglecting (i) the mixed-derivative term, since it is generally much smaller than the dominant terms, and (ii) gravity from spheroidal components, since their vertical force is much smaller than that from the disc. Hence, equation (24), which is obtained under these approximations, gives a good description of the vertical velocity dispersion σ_z of a stellar disc following a modified Kuzmin model.

In Fig. 6, we plot the profiles $\sigma_z(z)$ for our four comparison models for $h = 0.1s$ at different radii R . Consider first the sech^2 model (green in Fig. 6), which according to simple one-dimensional theory should produce a constant $\sigma_z^2 = 8\pi Gh^2\rho(R, 0)$ (Spitzer 1942, see also problem 4.21 of Binney & Tremaine 2008). At small $|z|$, this model indeed has near-constant σ_z (though not at the value expected from one-dimensional theory) but typically does not remain constant with height. These deviations are mainly owed to the departure from the assumption (used in the simple theory) of a reduced, one-dimensional Poisson equation, $4\pi G\rho = \partial^2\Phi/\partial z^2$.

All the models with an exponential vertical profile asymptote to very similar σ_z profiles at large $|z|$, but differ at small $|z|$. The purely exponential model shows a sharp minimum for σ_z , which is reminiscent of the profile observed in the Solar neighbourhood (Fuchs et al. 2009), while the cored exponential has a less pronounced and smooth minimum.

The MN model has a completely different σ_z profile than the exponentially declining models and reaches much larger values with maxima not captured in Fig. 6 (except for $R = 0$). This deviation is hardly due to the different gravity, but mainly owed to the shallower den-

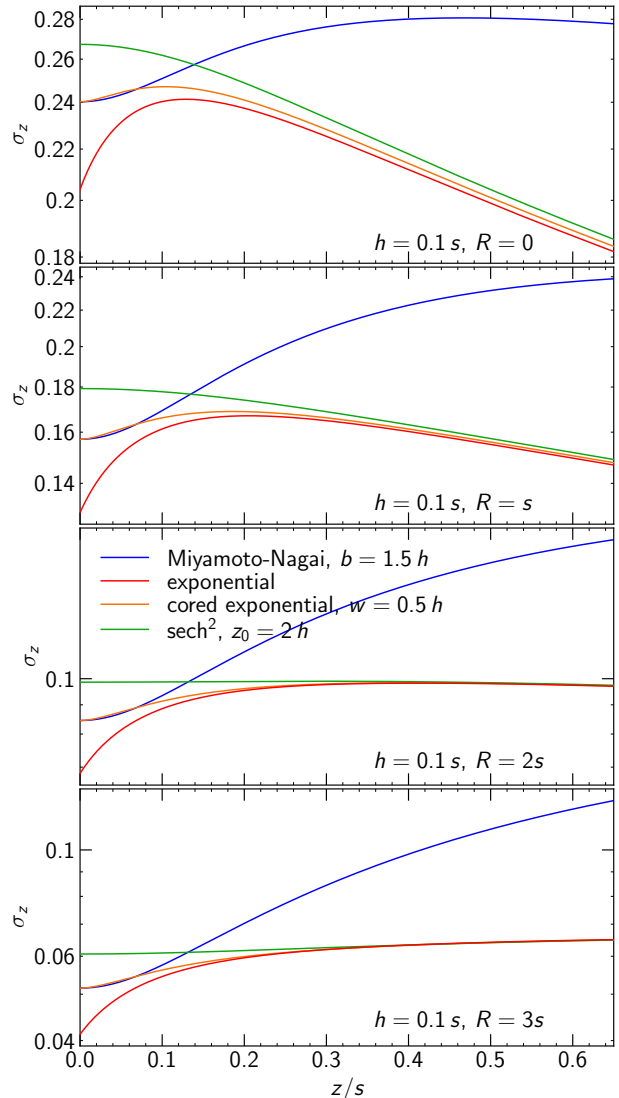


FIG. 6. — Profiles of the vertical velocity dispersion σ_z for self-gravitating modified Kuzmin models at different radii. Units are such that $GM = 1 = s$.

sity profile: σ_z is inflated by the high speeds of stars visiting from $z_{\max} \gg |z|$, but hardly present in exponentially decaying models.

5. DISCUSSION AND CONCLUSION

The main results of this study are the analytic mass models for thin discs with exponential or sech^2 vertical profile. These are obtained by modifying the razor-thin Kuzmin (1956) disc, very similar to how the Miyamoto & Nagai (1975; MN) model is constructed. In fact, many properties of the new models closely follow those of the MN model (with appropriately chosen parameters), so that the main difference is the vertical structure. Our approach can be used to construct modified Kuzmin models with arbitrary vertical profiles and in Appendix C we give the relations for a vertically near-Gaussian model.

The central density of an exponential vertical profile is significantly higher than for the MN or the sech^2 models (at the same surface density and exponential scale height). This higher central density results in a stronger

⁴ For small z_{\max} , $\bar{\Omega}_z$ computed at an average radius \bar{R} is a good approximation for the actual orbital frequency Ω_z .

vertical force at small $|z|$, and therefore also in higher vertical orbital frequencies Ω_z for stars with small maximal orbital height z_{\max} . This in turn affects various dynamical effects, such as the presence or absence of orbital resonances (between vertical and radial motion) and the degree of phase-mixing in the vertical phase space. Thus, the modelling of phenomena related to the vertical structure of galactic discs, such as z - v_z phase spirals and breathing or bending waves, are likely to be affected by the assumed vertical profile.

Another result of this study are the cored-exponential profiles, for which we also give analytic mass models constructed by modifying the Kuzmin (1956) disc. These models share with the exponential and sech^2 profiles the exponential decay with scale height h at large $|z|$, but differ at small $|z|$, where they possess a core of near-constant density with adjustable width $w \leq h$ (the sech^2 profile has core width $w = 2h$). As the precise vertical profiles of galactic discs near $z = 0$ are difficult to assess observationally and no theoretical foundations for either the exponential or sech^2 (or any other profile) exist⁵ (yet), these cored-exponential profiles are a useful addition to

the dynamicist's tool box and allow to study the effect of a density core of any width $w \leq h$.

Like the MN models, our new models are suitable bases for the construction of non-axisymmetric bar-shaped models by convolving them with a function $f(x)$ (Long & Murali 1992) and in fact, we have added them to the suite of mass models provided by the `discBar` code (Dehnen & Aly 2023).

One drawback of the MN models as well as our new models is the lack of realism of the radial profile, which closely follows that of the Kuzmin disc. While this profile resembles an exponential (with scale length $h_R = 2a/3$) over some radial range, a purely exponential profile would be desirable. Smith et al. (2015) have shown that three MN models can be combined to have a radially near-exponential surface density profile over four scale lengths. Of course, this approach is also available to our new models.

⁵ Of course, Spitzer (1942) obtained the sech^2 profile for an isothermal distribution under the assumption of one-dimensional dynamics and gravity. But neither are these assumption very good (Sarkar & Jog 2020), nor galactic discs expected to be isothermal.

REFERENCES

- Antoja T., et al., 2018, *Nature*, **561**, 360
 Binney J., Schönrich R., 2018, *MNRAS*, **481**, 1501
 Binney J. J., Tremaine S., 2008, *Galactic dynamics*. 2nd ed. Princeton, NJ, Princeton University Press
 Ciotti L., 2023, *MNRAS*, **525**, 2758
 Ciotti L., Pellegrini S., 1996, *MNRAS*, **279**, 240
 Dehnen W., Aly H., 2023, *MNRAS*, **518**, 2651
 Dehnen W., Binney J., 1998, *MNRAS*, **294**, 429
 Dehnen W., Hasanuddin 2018, *MNRAS*, **479**, 4720
 Dobbie P. S., Warren S. J., 2020, *OJA*, **3**, 5
 Evans N. W., Bowden A., 2014, *MNRAS*, **443**, 2
 Fuchs B., et al., 2009, *AJ*, **137**, 4149
 Jurić M., et al., 2008, *ApJ*, **673**, 864
 Kuijken K., Dubinski J., 1995, *MNRAS*, **277**, 1341
 Kuzmin G. G., 1956, *Astron. Zh.*, **33**, 27
 Long K., Murali C., 1992, *ApJ*, **397**, 44
 Miyamoto M., Nagai R., 1975, *PASJ*, **27**, 533
 Mosenkov A. V., Savchenko S. S., Smirnov A. A., Camps P., 2021, *MNRAS*, **507**, 5246
 Nagai R., Miyamoto M., 1976, *PASJ*, **28**, 1
 Plummer H. C., 1911, *MNRAS*, **71**, 460
 Rojas-Niño A., Read J. I., Aguilar L., Delorme M., 2016, *MNRAS*, **459**, 3349
 Sarkar S., Jog C. J., 2020, *MNRAS*, **499**, 2523
 Smith R., Flynn C., Candlish G. N., Fellhauer M., Gibson B. K., 2015, *MNRAS*, **448**, 2934
 Spitzer L., 1942, *ApJ*, **95**, 329
 Toomre A., 1963, *ApJ*, **138**, 385

APPENDIX

A. SURFACE DENSITY

Since $\Phi(R, z) = \Psi(R, \zeta)$ with $\nabla^2\Psi = 0$, we have

$$4\pi G\rho = \nabla^2\Phi = \frac{\partial^2\Phi}{\partial z^2} - \frac{\partial^2\Psi}{\partial\zeta^2}, \quad (\text{A1})$$

such that the face-on projections of the modified Kuzmin models have surface density

$$\Sigma(R) = \int_{-\infty}^{\infty} \rho dz = -\frac{1}{2\pi G} \int_0^{\infty} \frac{\partial^2\Psi}{\partial\zeta^2} dz = \frac{M}{2\pi} \int_0^{\infty} \left(\frac{2}{X^3} - \frac{3R^2}{X^5} \right) dz, \quad (\text{A2})$$

since $\partial^2\Phi/\partial z^2$ integrates to zero. In general, this integral cannot be expressed in closed form, though for the MN model Ciotti (2023) provides an expression involving elliptic integrals. Following Dehnen & Aly (2023), we compute this for any modifier $\zeta(z)$ numerically via Gauss Legendre quadrature after the substitution $t = z/\sqrt{z^2 + R^2 + s^2}$.

B. VELOCITY DISPERSION

To solve the Jeans equation for self-gravitating modified Kuzmin models, we use equation (A1) to obtain

$$\begin{aligned} \rho\sigma_z^2 &= \int_z^{\infty} \rho \frac{\partial\Phi}{\partial z} dz = \frac{1}{4\pi G} \left[\int_z^{\infty} \frac{\partial^2\Phi}{\partial z^2} \frac{\partial\Phi}{\partial z} dz - \int_{\zeta}^{\infty} \frac{\partial^2\Psi}{\partial\zeta^2} \frac{\partial\Psi}{\partial\zeta} d\zeta \right] = \frac{1}{8\pi G} \left[\int_z^{\infty} \frac{\partial}{\partial z} \left(\frac{\partial\Phi}{\partial z} \right)^2 dz - \int_{\zeta}^{\infty} \frac{\partial}{\partial\zeta} \left(\frac{\partial\Psi}{\partial\zeta} \right)^2 d\zeta \right] \\ &= \frac{1}{8\pi G} \left[\left(\frac{\partial\Psi}{\partial\zeta} \right)^2 - \left(\frac{\partial\Phi}{\partial z} \right)^2 \right] = \frac{1}{8\pi G} \left(\frac{\partial\Psi}{\partial\zeta} \right)^2 (1 - \zeta'^2) = \frac{GM^2}{8\pi} \frac{Z^2}{X^6} (1 - \zeta'^2). \end{aligned} \quad (\text{B1})$$

C. A GENERAL RECIPE FOR MODIFIERS

In order to obtain a vertical profile which closely follows a given functional form $f(|z|)$, a modifier $\zeta(z)$ satisfying all our conditions is constructed as follows. First, we define the integral $F(z) \equiv \int_0^z f(t) dt$. Then

$$\zeta(z) = \frac{F(\infty)}{f(0)} + \frac{1}{F(\infty)} \int_0^{|z|} F(t) dt, \quad \zeta'(z) = \text{sign}(z) \frac{F(|z|)}{F(\infty)}, \quad \zeta''(z) = \frac{f(|z|)}{F(\infty)}. \quad (\text{C1})$$

As an example, we apply this recipe to $f(z) = e^{-z^2/2w^2}$ for near-Gaussian vertical profiles, giving

$$\zeta_G = z \operatorname{erf} \frac{z}{\sqrt{2}w} + \sqrt{\frac{2}{\pi}} w \left[e^{-z^2/2w^2} + \frac{\pi}{2} - 1 \right], \quad \zeta'_G = \operatorname{erf} \frac{z}{\sqrt{2}w}, \quad \zeta''_G = \sqrt{\frac{2}{\pi}} \frac{1}{w} e^{-z^2/2w^2}. \quad (\text{C2})$$

For this modifier, $\zeta_G - \xi_G \geq 0$ everywhere, such that the resulting density is non-negative everywhere.